

## Island, Pit, and Groove Formation in Strained Heteroepitaxy

M. T. Lung,<sup>1</sup> Chi-Hang Lam,<sup>1</sup> and Leonard M. Sander<sup>2</sup>

<sup>1</sup>*Department of Applied Physics, Hong Kong Polytechnic University, Hung Hom, Hong Kong, China*

<sup>2</sup>*Michigan Center for Theoretical Physics, Department of Physics, Randall Laboratory, University of Michigan, Ann Arbor, Michigan 48109-1120, USA*

(Received 29 January 2005; published 18 August 2005)

We study the morphological evolution of strained heteroepitaxial films using a kinetic Monte Carlo method in three dimensions. The elastic part of the problem uses a Green's function method. Isolated islands are observed under deposition conditions for deposition rates slow compared with intrinsic surface roughening rates. They are hemispherical and truncated conical for high and low temperature cases, respectively. Annealing of films at high temperature leads to the formation of closely packed islands as in instability theory. At low temperature, pits form via a multistep layer-by-layer nucleation mechanism in contrast to the conventional single-step nucleation process. They subsequently develop into grooves, which are energetically more favorable.

DOI: [10.1103/PhysRevLett.95.086102](https://doi.org/10.1103/PhysRevLett.95.086102)

PACS numbers: 68.65.Hb, 81.16.Dn, 81.16.Rf

Epitaxial growth techniques have been used to deposit strained coherent films on substrates of a different material with a mismatched lattice constant. This is called heteroepitaxy. Many experiments have shown that beyond a threshold film thickness, an array of three-dimensional (3D) nanosized islands self-assembles under favorable growth conditions [1,2]. These results are of considerable interest since the islands behave as quantum dots and are expected to find applications in future microelectronic devices. The most intensively studied examples include Ge/Si(100) and more generally its alloy variant  $\text{Si}_{1-x}\text{Ge}_x/\text{Si}(100)$  [3–7]. The island morphology depends strongly and often nontrivially on the lattice misfit dictated by the Ge concentration as well as growth conditions including temperature and deposition rate. In addition, other interesting nanostructures including 3D pits, grooves, and quantum dot molecules composed of coupled islands and pits are also generated under appropriate conditions [8,9].

In this Letter, we report large scale 3D kinetic Monte Carlo simulations on the morphological evolution of strained layers. Our simulations generate morphologies very reminiscent of those observed under various growth or annealing conditions. We show that for high temperatures and low deposition rates the surface roughens via a linear instability [10], whereas for lower temperatures and higher rates islands, pits, and grooves form by nucleation. In particular, pits form by multistep nucleation. Some of these results were previously conjectured based on 2D results [11]. We should note that the simulation of strained layers is computationally challenging due to the long-range nature of elastic interactions. Previous atomistic simulations are limited to 2D [11–15] or submonolayer coverage [16] while genuine 3D simulations has become possible only very recently [17]. Continuum computations are less difficult but cannot reliably account for faceted surfaces and fluctuations, which are especially important at the early stage of roughening [18–20].

We model the film and substrate system by a simple cubic lattice of balls and springs [11,12]. The substrate consists of  $64 \times 64 \times 64$  atoms. Periodic boundary conditions in lateral directions and fixed boundary conditions for the bottom layer are assumed. The substrate has a lattice constant  $a_s = 2.72 \text{ \AA}$ , which gives an atomic density appropriate for crystalline silicon. The lattice constant  $a_f$  of the film is related to the lattice misfit  $\epsilon = (a_f - a_s)/a_f$ . Nearest neighboring (NN) and next nearest neighboring (NNN) atoms are directly connected by elastic springs with force constants  $k_1 = 2 \text{ eV}/a_s^2$  and  $k_2 = k_1$ , respectively. The elastic couplings of adatoms with the rest of the system are weak and are completely neglected.

Our algorithm imposes solid-on-solid conditions with atomic steps limited to at most one atom high. Every topmost atom in the film can hop to a different random topmost site within a neighborhood of  $l \times l$  columns with equal probability. We put  $l = 31$ . Decreasing the hopping range does not alter our results significantly. The hopping rate  $\Gamma_m$  of a topmost atom  $m$  follows an Arrhenius form

$$\Gamma_m = R_0 \exp\left[-\frac{n_{1m}\gamma_1 + n_{2m}\gamma_2 - \Delta E_m - E_0}{k_B T}\right]. \quad (1)$$

Here,  $n_{1m}$  and  $n_{2m}$  are the number of NN and NNN of atom  $m$ , respectively, while  $\gamma_1 = 0.085 \text{ eV}$  and  $\gamma_2 = \gamma_1/2$  are the corresponding bond strengths. The elastic energy of the hopping atom is denoted by  $\Delta E_m$  and will be explained later. Finally, we put  $E_0 = 0.415 \text{ eV}$  and  $R_0 = 2D_0/(\sigma a_s)^2$  with  $D_0 = 3.83 \times 10^{13} \text{ \AA}^2 \text{ s}^{-1}$  and  $\sigma^2 = l^2/6$ . This gives the appropriate adatom diffusion coefficient for silicon (100) [11]. Our choice of the ratios  $k_1/k_2$  and  $\gamma_1/\gamma_2$  maximizes the isotropy of the system.

The elastic energy,  $\Delta E_m$ , has to be repeatedly calculated during a simulation; this dominates the CPU time.  $\Delta E_m$  is defined as the difference in the strain energy  $E_s$  of the whole lattice at mechanical equilibrium when the site is

occupied minus that when it is unoccupied. Calculating  $E_s$  requires solving a long-range elasticity problem to obtain the atomic positions of every atom in the film and the substrate. We have found it possible to significantly speed up the calculation by applying an exact Green's function method. A method of this type was introduced by Tewary [21] in the context of point impurities. We generalized the technique to free surfaces in Ref. [11]. The result of these developments is that we can solve the elastic problem at a surface site using reduced equations involving only other surface atoms. Moreover, we use a surface coarsening scheme in which morphological details of the surface far away from atom  $m$  are averaged [11]. As a result, calculating  $\Delta E_m$  involves only about 160 effective particles and takes less than 1 s on a 3 GHz Pentium computer. Hopping events are then sampled using an acceptance-rejection algorithm aided by quick estimates of  $\Delta E_m$ , which enables a high acceptance probability. A simulation reported here typically involves  $10^6$  successful hopping events and takes 10 days to complete. We have considered large misfit and in some cases also high deposition rates so that the computations can be manageable.

We have simulated the deposition of films with 8% lattice misfit at temperature 1000 K and deposition rate  $R = 20\,000 \text{ ML s}^{-1}$ . Figure 1 shows the resulting morphology from a typical run at a nominal film thickness of 3 MLs. Isolated hemispherical islands are observed. Most of them nucleate when the nominal coverage is about 1 ML and then grow steadily as more atoms are deposited. Coarsening via exchange of atoms among islands (Ostwald ripening) also occurs. Some small islands shrink and vanish eventually. However, coalescence of islands is suppressed by their mutual elastic repulsion [22]. In fact, the edges of neighboring islands are often deformed to avoid each other.

In our simulations, as in experiments, the deposition rate has a substantial effect on surface morphology. At the rate considered above, island growth is limited by the supply of atoms. Individual islands have already relaxed to their equilibrium shapes. That is, deposition is slow relative to the formation dynamics and geometrical relaxation of islands. In contrast, at  $R > 5 \times 10^5 \text{ ML s}^{-1}$ , layers of

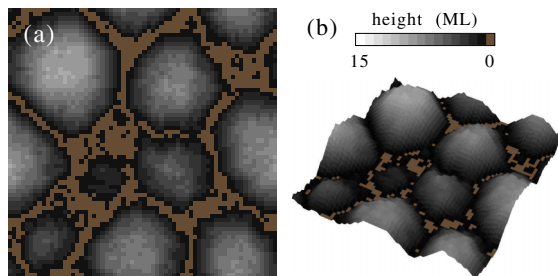


FIG. 1 (color online). Surface from simulation of deposition at 1000 K and  $20\,000 \text{ ML s}^{-1}$  in (a) top view and (b) 3D view. The gray scale shows the local height of the surface, and the exposed part of the substrate is shaded in brown.

atoms quickly accumulate before the resulting film roughens. We have observed from simulations of deposition at such rates as well as simulations of annealing that the development of a peak to peak roughness of, for example, 6 MLs takes about  $6 \mu\text{s}$ , which is identified as a strain induced roughening time. A deposition rate  $R > 5 \times 10^5 \text{ ML s}^{-1}$ , in fact, guarantees that the film is at least 3 MLs thick at  $6 \mu\text{s}$ . Thus, deposition and accumulation of atoms is fast compared to roughening. With an abundant supply of atoms, the roughening dynamics is similar to that for annealing except for a trivial vertical drift of the whole surface. We discuss annealing in detail next.

We have simulated annealing of initially flat films with 10 MLs of atoms and 6% lattice misfit at 1000 K. Figures 2(a)–2(c) show snapshots of the evolution. The 2D islands and pits first develop leading to a high step density [Fig. 2(a)]. At this point, the film is still relatively flat and highly stressed. The misfit has little impact on the morphology except for an enhancement of the step density due to a reduction of the effective step free energy. As the roughness increases, long-range elastic interactions begin to dominate and lead to the formation of 3D islands and pits with gentle slopes [Fig. 2(b)]. Subsequently, well developed 3D islands bounded by a network of grooves emerge [Fig. 2(c)].

The (100) surface studied above is not a true facet as is evident from the abundance of surface steps in Fig. 2(a). The temperature 1000 K must be above the surface roughening transition temperature. Similar surface properties are observed for temperatures down to 750 K, which is our estimate of the roughening temperature for our model at 6% misfit. Above the roughening temperature, the surface energy varies smoothly with the local inclination. The strain-induced roughening of such an unfaceted surface is

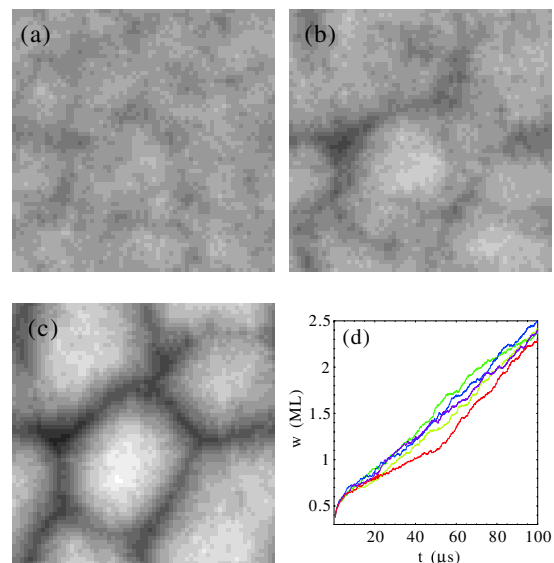


FIG. 2 (color online). Snapshots from annealing of an initially flat film at 1000 K at time (a)  $t = 20$ , (b) 50, and (c)  $100 \mu\text{s}$ , and (d) a plot of surface width  $w$  against  $t$  for 5 independent runs.

described by the Asaro-Tiller-Grinfeld instability theory [10], which predicts that random perturbations of the surface at sufficiently long wavelengths spontaneously amplify. The surface will gradually be dominated by modulations at the most unstable wavelengths.

The validity of the instability theory in describing our annealing results at 1000 K is further supported by the following observations. First, the sidewalls of the newly emerging islands are gentle and their inclinations increase gradually rather than abruptly. Moreover, the island base areas stay relatively constant. Further, we see in Fig. 2(d) the rms surface width  $w$  against the annealing time  $t$  for 5 independent runs. We observe that  $w$  increases steadily and the ensemble fluctuations are small as expected for barrierless processes. The morphological development also qualitatively resembles the initial evolution of  $\text{Si}_{1-x}\text{Ge}_x/\text{Si}(100)$  films at high temperature and low misfit [6]. Tersoff *et al.* have argued that the  $\text{Si}_{1-x}\text{Ge}_x(100)$  surface under these conditions is not a true facet [23] and theories based on unfaceted surfaces apply, although the suggestion is still controversial [7].

Next, we consider 600 K, which is well below the estimated roughening temperature of 750 K. Drastically different morphologies indicating distinct roughening mechanisms are observed. Figure 3 shows a surface at a nominal coverage of 2 MLs from a simulation of deposition at 8% misfit and  $10 \text{ ML s}^{-1}$ . We again observe isolated islands but they are now truncated cones. Most islands are out of equilibrium; their heights are limited by energy barriers for upper layer nucleation.

We have also simulated annealing at 600 K. Figures 4(a)–4(c) show three snapshots from a typical run. A large 2D island and a few smaller 2D pits first appear [Fig. 4(a)]. Later, 3D pits develop [Fig. 4(b)]. They become elongated and gradually turn into grooves [Fig. 4(c)]. Analogous 3D structures are also observed for deposition at rates fast compared to roughening.

A significant feature is that only part of the surface roughens even after a long annealing time in sharp contrast to the high temperature case. This indicates that the surface is a true facet below the roughening temperature. Its energy is a singular function of the slope and instability theory does not apply. Instead, nucleation theory is expected to describe the formation of 3D islands or pits [24,25].

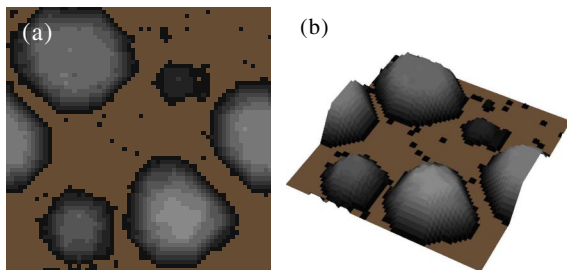


FIG. 3 (color online). Surface from simulation of deposition at 600 K and  $10 \text{ ML s}^{-1}$ .

According to this theory, an island or pit has to overcome an energy barrier associated with a critical volume before it can be stable. Figure 4(d) plots the rms surface width  $w$  against time from 5 independent runs during the early stage of roughening. There are large ensemble fluctuations supporting the relevance of nucleation processes. However, there exists no dominating jump in  $w$  associated with a single successful nucleation event after which  $w$  grows steadily. Instead, multiple relatively rapid increments between flat plateaus can be observed and are associated with the creation of lower layers in the dominant pits. Therefore, *single-step nucleation theory is invalid*. The formation of 3D pits in Fig. 4 and, in fact, also of the 3D islands in Fig. 3 instead follows a sequential layer-by-layer nucleation mechanism. Specifically, for a growing pit, atoms are ejected continuously while lateral expansion takes place at constant pit depth. Once the bottom becomes sufficiently large, nucleation of a further layer will be possible. Thus, the growth is based on the correlated processes of continuous lateral expansion and periodic sudden nucleation of deeper layers. The associated rates depend not only on the pit geometry but also on the presence of nearby islands or pits due to both exchange of atoms and elastic interactions. A detailed theoretical analysis is currently lacking.

The selection mechanism between islands and pits also deserves further explanation. Continuum elasticity theory shows that islands and pits with infinitesimal slopes relieve elastic energy equally well [24]. It is visually apparent that an up-down symmetry exists for surfaces in Fig. 2(a) and to a lesser extent also in Fig. 2(b). However, pits are increasingly favored energetically compared to islands as local slopes become steeper [26]. At low temperatures, the energy difference is already significant for single layered structures. Specifically, asymmetry between 2D islands

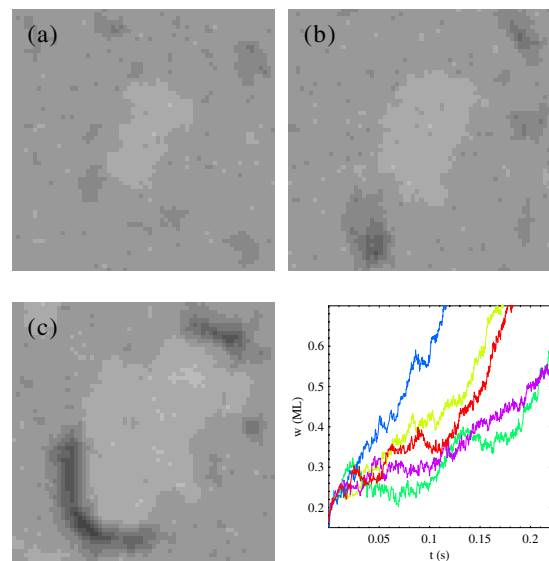


FIG. 4 (color online). Snapshots from annealing of an initially flat film at 600 K at time (a)  $t = 0.1$ , (b) 0.15, and (c) 0.22 s, and (d) a plot of  $w$  against  $t$  for 5 independent runs.

and pits is already apparent in Fig. 4(a). There is typically one dominant island but a few smaller pits. This is because the lower energy of pits also implies a lower nucleation barrier. Pits can hence nucleate more quickly and are more abundant. Because new islands are not nucleated, the existing one absorbs all the ejected atoms and grows quickly. Furthermore, the better stability of pits also explains the development of 3D pits rather than 3D islands in Figs. 4(b) and 4(c). We have observed 3D islands in Fig. 3 only for slow deposition. This is because with this slow deposition rate, 3D islands are already able to develop before a thick enough film can be formed to accommodate the pits [11]. Experimentally, the selected structure also turns from 3D islands to 3D pits upon lowering the temperature and increasing the deposition rate [8].

An interesting transition from pits to grooves is also observed in Figs. 4(b) and 4(c). It occurs when pits are about 3 layers deep with about 150 atomic vacancies. For shallow pits, a square base is energetically preferred to a rectangular one [24]. This explains the more rounded shapes of the pits in Fig. 4(b). As the pits enlarge, their sidewalls also become steeper to relieve the stress more efficiently. Grooves are then energetically preferred to rounded pits because their linear extents are larger and can lead to stress relief over a much wider region. By considering simple pits and grooves of 3 layers deep, we have found numerically that grooves start to have a lower total energy at a size of about 60 vacancies. This verifies the energetic origin of the pit to groove transition, although a precise determination of the transition point requires a full calculation of the free energies. The formation of grooves in Fig. 4(c) is further enhanced by the stress around a 2D island. The presence of a neighboring island is not essential as we have also observed pits turning into grooves far away from any islands. Grooves are also observed in experiments from the annealing of pits. The transition has been attributed to kinetic effects based on (105) faceted sidewalls of the pits [9], which is not supported by our simulations.

In conclusion, we have applied a kinetic Monte Carlo method in 3D to study morphological structures generated from deposition and annealing of strained heteroepitaxy. Under deposition conditions, morphologies depend dramatically on whether deposition is slow compared to the intrinsic strain induced roughening rate of the surface as in the 2D case [11]. For slow deposition, isolated islands result, and their formation and development are limited by the supply of atoms. In contrast during fast deposition, 3D structures form only after layers of atoms have accumulated and are similar to those from annealing of initially flat films. Also, morphologies from annealing show a strong dependence on temperature, which determines whether the initial surface is faceted. Upon annealing at high temperature, unfaceted surfaces develop arrays of 3D islands via the Asaro-Tiller-Grinfeld instability. In contrast, faceted surfaces at low temperature develop 3D pits

via a layer-by-layer nucleation mechanism. The pits later turn into grooves. The selection mechanisms between islands and pits as well as between pits and grooves are of energetic origin.

We thank J. A. Floro for helpful discussions. This work was supported by HK RGC, Grant No. PolyU-5289/02P. L. M. S. is supported in part by NSF Grant No. DMS-0244419.

- 
- [1] V. A. Shchukin and D. Bimberg, *Rev. Mod. Phys.* **71**, 1125 (1999).
  - [2] P. Politi *et al.*, *Phys. Rep.* **324**, 271 (2000).
  - [3] Y.-W. Mo, D. E. Savage, B. S. Swartzentruber, and M. G. Lagally, *Phys. Rev. Lett.* **65**, 1020 (1990).
  - [4] D. E. Jesson, K. M. Chen, S. J. Pennycook, T. Thundat, and R. J. Warmack, *Phys. Rev. Lett.* **77**, 1330 (1996).
  - [5] A. Vaillonis, B. Cho, G. Glass, P. Desjardins, David G. Cahill, and J. E. Greene, *Phys. Rev. Lett.* **85**, 3672 (2000).
  - [6] J. A. Floro *et al.*, *Phys. Rev. B* **59**, 1990 (1999).
  - [7] P. Sutter, P. Zahl, and E. Sutter, *Appl. Phys. Lett.* **82**, 3454 (2003).
  - [8] J. L. Gray, R. Hull, and J. A. Floro, *Appl. Phys. Lett.* **81**, 2445 (2002).
  - [9] J. L. Gray, R. Hull, and J. A. Floro, *Appl. Phys. Lett.* **85**, 3253 (2004).
  - [10] M. A. Grinfeld, *J. Nonlinear Sci.* **3**, 35 (1993).
  - [11] C. H. Lam, C. K. Lee, and L. M. Sander, *Phys. Rev. Lett.* **89**, 216102 (2002).
  - [12] B. G. Orr, D. A. Kessler, C. W. Snyder, and L. M. Sander, *Europhys. Lett.* **19**, 33 (1992).
  - [13] K. E. Khor and S. Das Sarma, *Phys. Rev. B* **62**, 16657 (2000).
  - [14] F. Much and M. Biehl, *Europhys. Lett.* **63**, 14 (2003).
  - [15] J. L. Gray, R. Hull, C. H. Lam, P. Sutter, J. L. Means, and J. A. Floro (unpublished).
  - [16] M. Meixner, E. Schöll, V. A. Shchukin, and D. Bimberg, *Phys. Rev. Lett.* **87**, 236101 (2001).
  - [17] G. Russo and P. Smereka (unpublished).
  - [18] W. H. Yang and D. J. Srolovitz, *Phys. Rev. Lett.* **71**, 1593 (1993).
  - [19] Y. W. Zhang, A. F. Bower, and P. Liu, *Thin Solid Films* **424**, 9 (2003).
  - [20] A. Ramasubramaniam and V. B. Shenoy, *J. Appl. Phys.* **95**, 7813 (2004).
  - [21] V. K. Tewary, *Adv. Phys.* **22**, 757 (1973).
  - [22] D. E. Jesson, T. P. Munt, V. A. Shchukin, and D. Bimberg, *Phys. Rev. B* **69**, 041302 (2004).
  - [23] J. Tersoff, B. J. Spencer, A. Rastelli, and H. von Känel, *Phys. Rev. Lett.* **89**, 196104 (2002).
  - [24] J. Tersoff and F. K. LeGoues, *Phys. Rev. Lett.* **72**, 3570 (1994).
  - [25] M. Bouville, J. M. Millunchick, and M. L. Falk (unpublished).
  - [26] D. Vanderbilt and L. K. Wickham, in *Evolution of Thin-Film and Surface Microstructure*, edited by C. V. Thompson *et al.*, MRS Symposia Proceedings No. 202 (Materials Research Society, Pittsburgh, 1991), p. 555.